

See discussions, stats, and author profiles for this publication at: <https://www.researchgate.net/publication/262144303>

A Minimal Cluster Model of Valence Electrons in Adatom-Assisted Adsorbed Molecules: NCH₃/Cu(110) and OCH₃/Cu(110)

ARTICLE *in* THE JOURNAL OF PHYSICAL CHEMISTRY C · APRIL 2014

Impact Factor: 4.77 · DOI: 10.1021/jp411066x

READS

74

3 AUTHORS, INCLUDING:



Michitoshi Hayashi

National Taiwan University

199 PUBLICATIONS 2,151 CITATIONS

SEE PROFILE

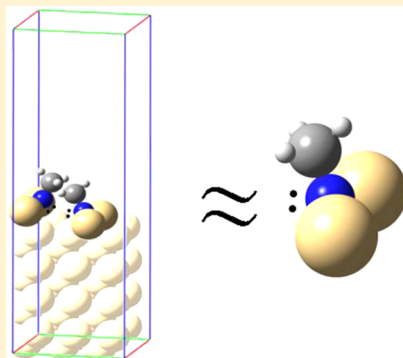
A Minimal Cluster Model of Valence Electrons in Adatom-Assisted Adsorbed Molecules: NCH₃/Cu(110) and OCH₃/Cu(110)

Po-Tuan Chen, Woei Wu Pai,* and Michitoshi Hayashi*

Center for Condensed Matter Sciences, National Taiwan University, Taipei 106, Taiwan

S Supporting Information

ABSTRACT: In this study, we found that the local density of states and ionization energy spectrum of the valence electrons of methylnitrene (NCH₃) adsorbed on Cu(110) can be calculated from molecular orbital calculations of a simple artificial isolated NCH₃–Cu₂ molecular cluster in which the two Cu atoms form bonds to the N atom. Such a NCH₃–Cu₂ cluster represents the basic structural unit of a NCH₃ molecule adsorbing on a Cu double-added-row structure. This finite NCH₃–Cu₂ cluster structure is not optimized as a single system but is extracted directly from an optimized surface structure obtained by density functional theory with periodic boundary conditions. With this approach, we obtained excellent agreement between the measured ultraviolet photoemission spectra (UPS) and the theoretical calculation results. To further examine this minimal cluster concept, we analyzed methoxy (OCH₃) adsorption on Cu(110) and found a OCH₃–Cu₃ cluster structure. On the basis of this structure, we calculated UPS and also obtained substantial agreement with the experimental UPS. These results may indicate that, when substrate adatoms bridge the adsorption of a molecule and a surface, a small cluster consisting of the adsorbate and the neighboring bonding substrate adatoms suffices to describe the electronic structure of the valence electrons of the adsorbates.



INTRODUCTION

Surfaces have intrinsic structures, physical and chemical properties, and functions that are quite different from those of the bulk systems. The atoms at the surface are coordinatively unsaturated; thus, chemical adsorptions and chemical reactions can readily take place. Such surface modifications may induce rearrangements of atoms at the surface involving surface reconstruction and/or relaxations. Thus, one can anticipate that the geometrical and electronic structures of adsorbed molecules are quite different from those of the molecules in the gas phase. In particular, during reconstruction, if a few adatoms are involved, it should be important to understand the effects of the adatoms on the electronic structures of the adsorbed molecules and the surface. If a simple molecule takes part in such an adatom-involved adsorption, a clear signature of electronic structure modification of the adsorbed molecule may be deduced and analyzed. In this study, we will select methylnitrene (NCH₃) on Cu(110) as our probing system. Characterizing this system is fundamentally significant to understand several catalytic processes.^{1–3} Previously, it has been found that azomethane (CH₃N=NCH₃) adsorbed on Cu(110) in ultrahigh vacuum decomposes into NCH₃ at room temperature, and the stable existence of the decomposed NCH₃ on Cu(110) has been identified by vibrational spectra,⁴ temperature-programmed desorption,⁴ UPS,⁴ and scanning tunneling microscopy (STM).^{5,6} Moreover, quite recently, we have proposed the most plausible structure of this adsorption system based on density functional theory (DFT) calculations and STM imaging.¹ We discovered that a key feature of its

bonding is that each NCH₃ does not form a bond to the flat Cu(110) directly but that to the Cu adatoms through the N–Cu bonds. The N atom coordinates with the two Cu atoms, the methyl group, and the lone electron pair of the N atom in a tetrahedral fashion. More structure details are discussed below. One can view that the two Cu adatoms weaken the interaction between the NCH₃ and the flat Cu(110). Moreover, the UPS spectra of the adsorbed and the gas-phase NCH₃ differ significantly.⁴ This indicates significant interaction between NCH₃ and Cu, i.e., the Cu adatoms and/or those at Cu(110). A question about the Cu adatoms' role on the valence electron configurations of NCH₃ is, therefore, highly relevant.

We first briefly introduce methylnitrene NCH₃. It is the simplest alkylnitrene. Gas-phase NCH₃ adopts a C_{3v} symmetry and a triplet state with two unpaired electrons, forming a diradical that participates in a number of organic chemical reactions.^{7,8} NCH₃ is also a Jahn–Teller active and short-lived species. It quickly transforms into HN=CH₂,^{9–11} which is of considerable interests because it is connected to the origin of life.^{12,13} The structure and vibrational spectra of a triplet NCH₃ have been examined fully.^{14–20} Yarkony et al.⁹ reported theoretical results of the electron configuration of a triplet NCH₃, i.e., 1a₁²a₁²3a₁²4a₁²1e⁴5a₁²2e². More ab initio calculations of the electronic states of NCH₃ were subsequently

Received: November 11, 2013

Revised: April 15, 2014

Published: April 18, 2014



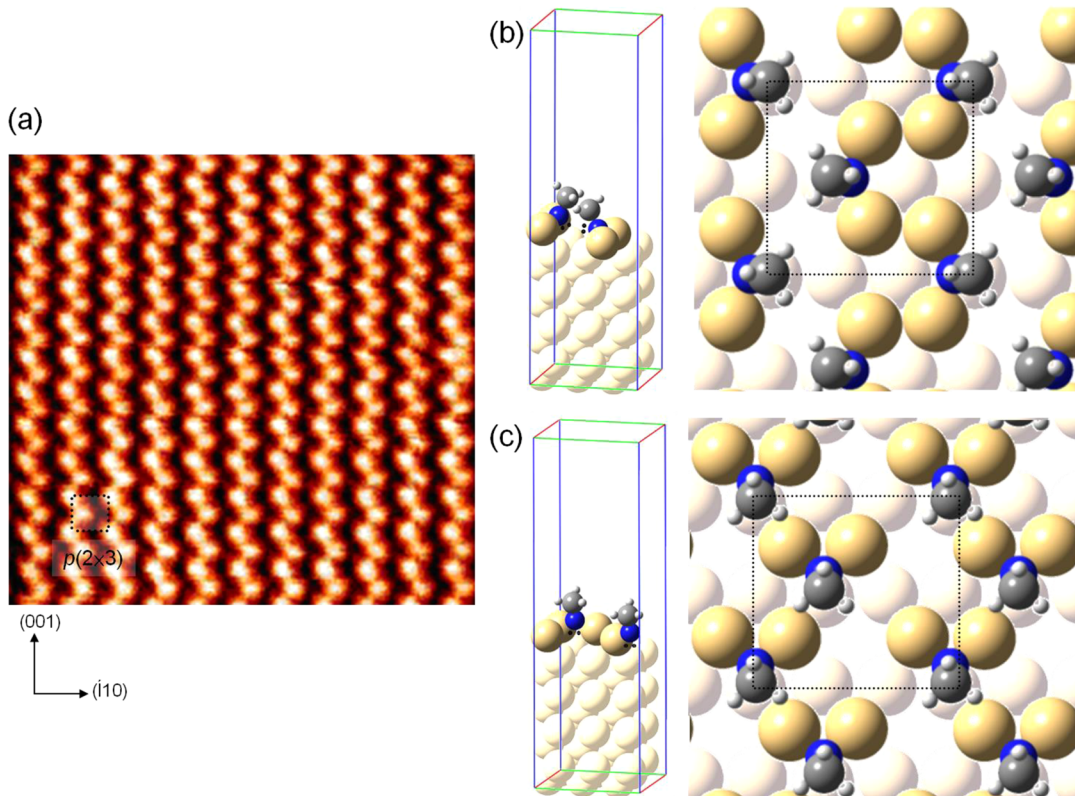


Figure 1. Experimental images and proposed structures of NCH_3 adsorbed on $\text{Cu}(110)$. (a) A typical $p(2 \times 3)$ NCH_3 STM image. We used VASP to check that the bright features are contributions from CH_3 groups. Imaging conditions: sample $V = 0.03$ V, $I = 0.13$ nA. Image size: 8 nm \times 8 nm. (b) A top view of the “double-row” Slab A model and the DFT supercell. (c) A top view of the “dimer” Slab B model and the DFT supercell. Also see in ref 1.

reported.^{10,11,21–23} In addition, ionization of NCH_3 has been examined by photoelectron spectroscopy.^{24,25}

Multiconfiguration molecular orbital (MO) methods^{24,25} are applicable for simulating quantitative values of n th ionization energy (IE), e.g., ionized from HOMO, HOMO-1, and so on, because such methods can take into account several correction terms, for instance, $(N - 1)$ electron orbital relaxations, to Koopman’s theorem. In addition, ab initio simulations of UPS for adsorbed molecules should take into account the details of adsorption geometry, including that of the molecule and the substrate. Thus, a cluster model can be considered. A surface is typically represented by a cluster of up to several tens of substrate atoms, and adsorbates are then added to this cluster. Finally, MO wave functions are used to determine properties of the whole adsorbate–substrate system. This approach is effective for treating adsorbate–substrate interaction and has been used extensively to provide valuable insights to chemisorptions and catalysis,^{26,27} and to analyze the electronic states of adsorbates.²⁸ However, the required cluster size to properly represent adsorbates on a surface is not known a priori, and the calculation of ionization spectra is often formidable for large size clusters or periodical metallic systems. The cluster model approach also yields cluster-size dependent properties,²⁹ and proper convergence must be carefully checked. However, since an adsorbed NCH_3 on $\text{Cu}(110)$ is separated from the flat surface by two immediate-bonding Cu adatoms, the two Cu adatoms may weaken the interaction between the adsorbed NCH_3 and the flat $\text{Cu}(110)$ surface, and a minimal cluster, e.g., $\text{NCH}_3\text{–Cu}_2$, may be used for accurate IE calculations. If this is the case, one can view that the interacting

valence electrons are localized within a rather small cluster. In particular, the problem of computation demand for large cluster MO calculations is also alleviated. Characterization of the ultraviolet photoemission spectra (UPS) and ionized state electronic structures of organic compounds interacting with metal surfaces will readily be performed, which should be relevant to the fields of organic optoelectronics and molecular devices.

METHOD

We used a plane-wave DFT with the PW91 generalized gradient approximation³⁰ of the Vienna Ab initio Simulation Package (VASP)^{31–33} for structure calculations. A unit cell consisting of an eight-layer Cu slab and a vacuum gap > 10 Å was used in which the upper six Cu layers were fully relaxed. Calculations were performed with spin-polarized conditions. An energy cutoff of 400 eV and a $5 \times 5 \times 1$ Monkhorst–Pack grid³⁴ were adopted.

The G2³⁵ or the G2+³⁶ method is appropriate for the IE calculation of the NCH_3 radical.²⁴ To calculate the IE of NCH_3 on the $\text{Cu}(110)$ surface, a few approximations were made: (1) a vertical transition during ionization without any geometrical change. Thus, single-point calculations were performed for the IE. (2) The core electrons of the Cu atom do not participate in ionization below 10 eV, and an effective core potential of the LANL2DZ^{37–39} basis was used for Cu. (3) CISD was adopted to include the final state interaction. The C, N, O, and H atoms were treated by the 6-311+G(d,p) basis set. In order to enhance calculation accuracy, we also took into account the

Table 1. Geometries of Cluster A, Cluster B, and Self-Optimized NCH₃-Cu₂^a

	Cluster A ¹	Cluster B ¹	self-optimized NCH ₃ -Cu ₂ cluster ^b
d(Cu-Cu)	3.39	2.64	2.60
d(Cu-N)	1.94	1.89	1.86
d(N-C)	1.47	1.47	1.47
d(C-H)	1.10	1.10	1.10
∠(Cu-N-Cu)	121	88.0	88.0
∠(C-N-Cu)	117	129	116

^aUnits: bond distance, Å; bond angle, degrees. ^bCalculations based on B3LYP level; N, C, and H are treated by the 6-31+G(d,p) basis, while Cu is treated by the LANL2DZ basis.

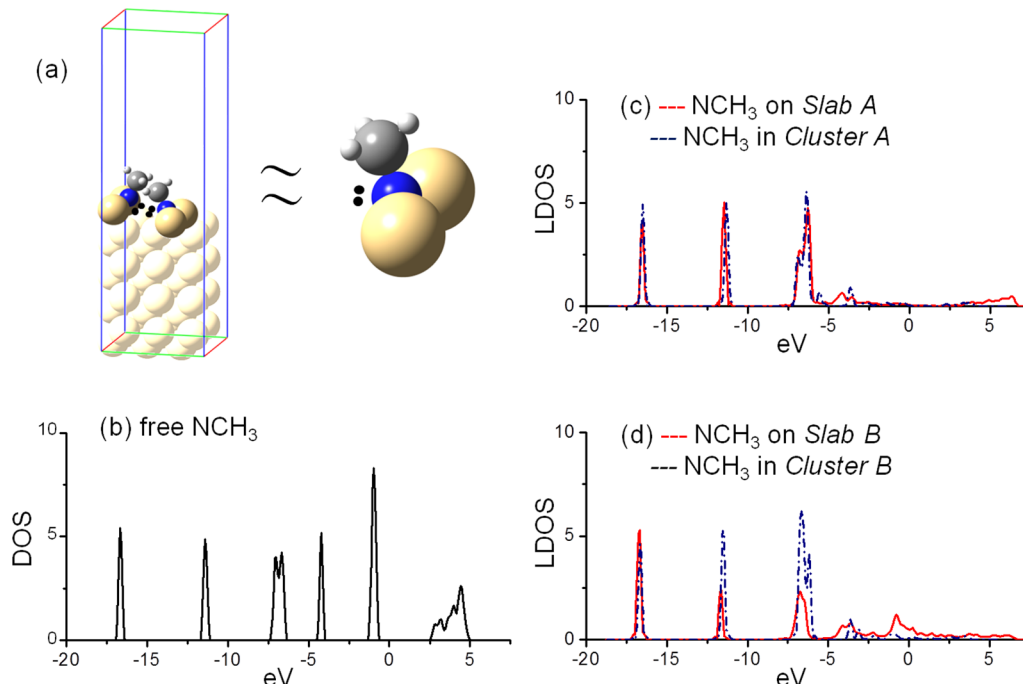


Figure 2. (a) The NCH₃-Cu₂ “molecule” (Cluster A) is constructed by removing all of the Cu atoms except the two adatoms that are directly bonded to NCH₃, from the Slab A model. The double dot denotes the lone electron pair on N. (b) The DOS of a free NCH₃ molecule. (c) The NCH₃ LDOSs of the Slab A and the Cluster A models. (d) The NCH₃ LDOSs of the Slab B and the Cluster B models. The DOSs of free NCH₃ in (b) and Clusters A and B in (c, d) are shifted by -1.0, -0.2, and -0.5 eV, respectively, to align with the state at ~ -17 eV in the slab models. The free NCH₃ DOS uses Gaussian smearing, and the slab and cluster model LDOSs use Methfessel-Paxton order 1 smearing.

basis set corrections [$\Delta E(2\text{df})$ and $\Delta E(3\text{df},2\text{p})$] in G2+³⁶ for the C, N, O, and H atoms

$$\begin{aligned} \Delta E(2\text{df}) &= [\text{MP4}/6-311+\text{G}(2\text{df},\text{p})] \\ &\quad - [\text{MP4}/6-311+\text{G}(\text{d},\text{p})] \end{aligned}$$

$$\begin{aligned} \Delta E(3\text{df},2\text{p}) &= [\text{MP2}/6-311+\text{G}(3\text{df},2\text{p})] \\ &\quad - [\text{MP2}/6-311+\text{G}(2\text{df},\text{p})] \end{aligned}$$

and a higher level correlation correction [$\Delta E(\text{HLC})$]

$$\begin{aligned} \Delta E(\text{HLC}) &= -0.13088(\text{no. of } \beta \text{ valence electrons}) \\ &\quad - 0.00517(\text{no. of } \alpha \text{ valence electrons}) \end{aligned}$$

Therefore, the electronic energy is given by the sum of these corrections

$$\begin{aligned} E &= \text{CISD}/6-311+\text{G}(\text{d},\text{p}) + \Delta E(2\text{df}) + \Delta E(3\text{df},2\text{p}) \\ &\quad + \Delta E(\text{HLC}) \end{aligned}$$

As a controlled group, the geometry of the self-optimized NCH₃-Cu₂ cluster in gas phase was calculated by B3LYP; the Cu atoms were treated by the LANL2DZ basis, while the C, N, and H atoms were treated by 6-311+G(d,p). Then, the MO calculations and the self-optimization of NCH₃-Cu₂ were performed with the GAUSSIAN 03 package.⁴⁰

RESULTS AND DISCUSSION

Geometry of NCH₃ Adsorbing on Cu(110) Surface with Adatoms. We now briefly summarize our proposed adsorption geometry of NCH₃ on Cu(110).¹ In the previous STM study,^{8,6} we observed that NCH₃ molecules aggregate to form p(2 × 3) islands. Each p(2 × 3) unit cell consists of two NCH₃ molecules that order in a zigzag arrangement, as shown in Figure 1a. The presence of adsorbate-induced surface reconstruction is evident from pit formation;^{41,42} it showed that a 1:2 NCH₃:Cu(adatom) stoichiometry must hold. Low energy electron diffraction and energetics consideration demand a *pmg* adsorption symmetry. Several possible adsorption structures were tested with DFT-calculated and experimental STM images.¹ Two final plausible structures were

then obtained. In Figure 1b (Slab A: the “double-row” model), each NCH_3 molecule forms bonds to the two closest Cu adatoms alternatively along a Cu added double row, with the imaged CH_3 groups tilted toward the neighboring vacant (missing) rows. In Figure 1c (Slab B: the “dimer” model), each NCH_3 with a tilted CH_3 group forms a bond to a Cu adatom dimer. These two structures are similar in that the two unpaired electrons of NCH_3 form bonds to two Cu adatoms. The two models are different in their local bonding geometry as the distance between the two Cu adatoms bonded to NCH_3 is $\sqrt{2}a$ and a for Slabs A and B, respectively (where a is the close-packed Cu–Cu distance, ca. 2.56 Å). The DFT calculations indicated that the double-row model is lower in energy than the dimer model by as much as 0.16 eV per $p(2 \times 3)$ unit cell. If Slab A and B structures coexist, Boltzmann distribution suggests a population ratio at room temperature of Slab A/B $\sim 500/1$. We, therefore, believe that Slab A is the dominant configuration.

LDOS of the Minimal Clusters. An interesting view in both of the above-mentioned models is that a new molecular moiety, $\text{NCH}_3\text{--Cu}_2$, adsorbs on the flat Cu(110). Can the local electronic structure of an adsorbed NCH_3 on Cu(110) be modeled with an isolated $\text{NCH}_3\text{--Cu}_2$? To test this conjecture, we first examined the local density of states (LDOS). The geometries of Slab A and Slab B were taken directly from ref 1. The geometrical parameters of Cluster A and Cluster B are shown in Table 1. Two types of $\text{NCH}_3\text{--Cu}_2$ clusters (named Cluster A/B) were considered. For example, Cluster A is simply Slab A with the flat Cu(110) and all, but one, $\text{NCH}_3\text{--Cu}_2$ removed, as illustrated in Figure 2a. The coordinates of Cluster A are fixed as the Slab A is reduced to Cluster A. Cluster B is obtained in the same way. Previously, a similar approach was also used for a MgO-supported Au_8 cluster on a Ag surface.²⁸

We compared the LDOSs of the slab and cluster models. In Figure 2c, the high similarity of LDOSs of NCH_3 in Slab A and Cluster A suggests that the electronic hybridization between the Cu adatoms and the NCH_3 overwhelms the weaker bonding of NCH_3 with the Cu(110) substrate. The NCH_3 LDOSs of Slab B and Cluster B (Figure 2d) are in less agreement, but it is fair to say that the LDOS is not very sensitive to minute structural differences of NCH_3 in the slab and cluster models. Figure 2b shows the DOS of a free NCH_3 molecule; it is quite different from those of NCH_3 on Slab A or Slab B, therefore hinting of substantial interactions between NCH_3 and Cu.

Ionization Energy of $\text{NCH}_3/\text{Cu}(110)$. In addition to LDOS, IE values were tested against the two cluster models. Our results show that, in contrast to LDOS, simulated IE values are sensitive to slight variations of the Cluster A and B structures. Theoretical and the experimental IE values are compared in Figure 3 and Table 2. The correct Cluster A model nicely reproduces the experimental data, whereas the Cluster B model is clearly inconsistent. Ionization energies are quite sensitive to subtle differences in geometrical parameters of the two clusters, and almost a 1 eV difference was obtained for the first ionization energies.

Using the $\text{NCH}_3\text{--Cu}_2$ cluster model, we find that the ground state of $\text{NCH}_3\text{--Cu}_2$ is a singlet instead of a triplet, unlike a gas-phase NCH_3 . Bonding to two Cu adatoms removes the intrinsic Jahn–Teller instability of NCH_3 , and the degenerate half-filled degenerate HOMOs split into an occupied HOMO and an unoccupied LUMO. The singly ionized configuration of a singlet NCH_3 is either a doublet or a quartet. Our calculations show that at least the first four ionization configurations are

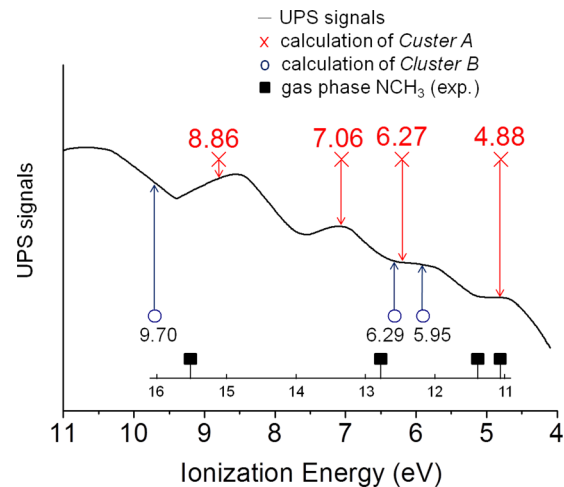


Figure 3. Comparison of the calculated ionization energies for Cluster A, Cluster B, the experimental UPS of ref 4, and gas-phase NCH_3 (experiment) of ref 24.

doublets. In order to roughly illustrate the major contribution of the levels, we used Hartree–Fock MOs and Koopman’s theorem as shown in the Supporting Information (S1).

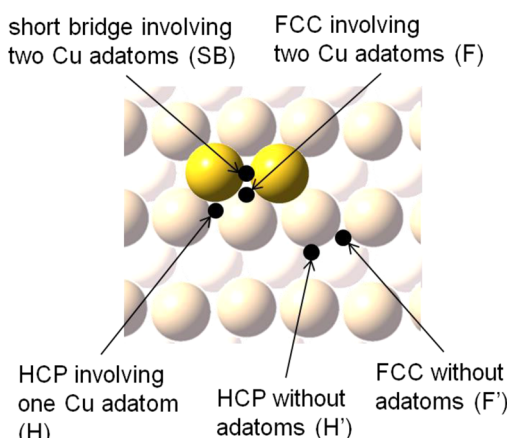
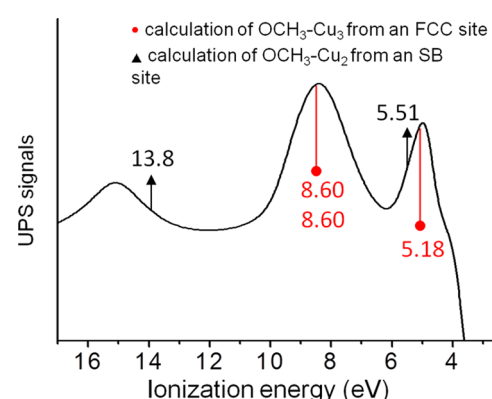
Finally, we note that, if the $\text{NCH}_3\text{--Cu}_2$ structure is not taken directly from the plane-wave DFT results but is fully optimized as in a typical cluster calculation, the IEs (5.96, 6.30, and 9.10 eV) are completely different from the experimental values. This illustrates the key merit of the minimal cluster approach; i.e., a properly structure-optimized minimal cluster (by DFT), if embedding the essential adsorbate–substrate interactions,¹ seems capable of predicting electronic properties of the valence electrons of adsorbates such as the ground-state LDOS or the excited-state IE spectra with high accuracy.

The IEs of the self-optimized $\text{NCH}_3\text{--Cu}_2$ cluster (5.96, 6.30, and 9.10 eV) are, on the other hand, similar to those of Cluster B (5.95, 6.29, and 9.70 eV). We reason that this is due to the similarities in their structures, as shown in Table 1. We propose that the distance of direct-binding Cu adatoms has a major influence on the ionic state; for example, this distance in Cluster B or the self-optimized $\text{NCH}_3\text{--Cu}_2$ shows only 0.04 Å deviation. A comparison of the LDOS of NCH_3 in the self-optimized $\text{NCH}_3\text{--Cu}_2$ and in Cluster B is shown in the Supporting Information (S2).

Ionization Energy of $\text{OCH}_3/\text{Cu}(110)$. We employed the minimal cluster approach to another important species, methoxy (OCH_3), on Cu(110). Methoxy is a key reaction intermediate in the partial oxidation of methanol on Cu(110) to produce formaldehyde (H_2CO). The adsorption structure of OCH_3 on Cu(110) has been debated intensively. A recent photoelectron diffraction and DFT study^{43,44} has suggested that the most favorable adsorption site for OCH_3 is the short bridge (SB) site over a Cu adatom pair; see Figure 4. From this bonding configuration, a $\text{OCH}_3\text{--Cu}_2$ minimal cluster was used for IE calculations, giving peaks at 5.51 and 13.82 eV. These IEs do not match well the observed ionization bands of ~ 5.0 and ~ 15.2 eV, and miss the intense IE peak at ~ 8.5 eV; see Figure 5. Because oxygen has one more electron than nitrogen, a local bonding configuration of $\text{OCH}_3\text{--Cu}_3$ seems to make a better chemical sense. Indeed, a 3-fold hollow adsorption geometry is known for $\text{OCH}_3/\text{Cu}(111)$.⁴⁵ Therefore, we examined OCH_3 adsorption on various 3-fold hollow sites on Cu(110). Four possible 3-fold hollow sites are FCC and HCP sites on (111)–

Table 2. Comparison of the Calculated Ionization Energies with the Modified G2+ and Experimental Values^a

experiment of NCH ₃ /Cu(110)	IE from minimal cluster - Cluster A	IE from minimal cluster - Cluster B	IE from self-optimized NCH ₃ -Cu ₂ cluster
4.8	4.88	5.95	5.96
5.7	6.27	6.29	6.30
7.1	7.06		
8.6	8.86	9.70	9.10

^aUnit: eV.**Figure 4.** Top view of the short bridge (SB) and the 3-fold hollow sites (F, H, F', H') on Cu(110). The yellow spheres denote Cu adatoms.**Figure 5.** Comparison of the calculated ionization energies for a OCH₃-Cu₃ cluster and the experimental UPS (“d-a” curve of Figure 7 of ref 46; also see Figure 4c of ref 47). The degeneracy of the HOMO-1 level results in two overlaid peaks near 8.6 eV.

microfacets without involving Cu adatoms (F', H' sites) and FCC and HCP sites on (111)-microfacets involving Cu adatoms (F, H sites), as shown in Figure 4. Adsorption at F' and H' sites is less favorable than at F and H sites because of steric interactions between the adsorbate and the substrate. Our VASP calculations show that the adsorption energy is almost 0.14 eV lower at the F site than at the H site. Most importantly, the adsorption energy at the F site is also comparable (~0.02 eV less) to the adsorption energy at the SB site. More calculation details are in the Supporting Information (S3). For adsorption at the F sites, the O-C axis is nearly perpendicular to the local (111)-microfacet, as reported in ref 45. Therefore, our calculations suggest that the 3-fold FCC hollow site involving a Cu adatom pair (an F site) makes good sense and cannot be excluded. Incidentally, this F site geometry is not considered for the adsorption energy or the photoelectron

diffraction fitting in ref 44. Because of the small energy difference of adsorption at SB and F sites, they could also coexist on the surface.

We then used a OCH₃-Cu₃ cluster with the F site geometry from our DFT structure to calculate IE; see Figure 5. The first three calculated IE levels at 5.18, 8.60, and 8.60 eV match the experimental data closely.^{46,47} The two degenerate levels at 8.60 eV reflect the approximate C₃ local adsorption symmetry. If the structure relaxation is obtained from the OCH₃-Cu₃ cluster per se, the IE levels (5.35, 8.07, and 9.14 eV) are in less agreement with the experimental results. Further details of OCH₃ on the F site are discussed in the Supporting Information (S4 and S5). From the DFT energetics, the 3-fold hollow F site should not be disregarded. The finding that the OCH₃-Cu₃ minimal cluster reproduces the IE spectra suggests that the F site adsorption is plausible and its IE levels constitute a significant part of the observed UPS spectrum. In fact, the observed experimental UPS spectrum can be taken as a UPS spectrum of mixed OCH₃-Cu₃ and OCH₃-Cu₂ clusters. We suggest that our proposed F site OCH₃ adsorption needs to be reconciled with the SB site adsorption proposed earlier⁴⁴ in future experiments.

CONCLUSION

An interesting finding in our work is that MO methods applied to a surface adsorbate with its structure being optimized in periodic DFT slab calculations can predict the excited-state property of the valence electrons of the adsorbate such as IE that is not easy to obtain by DFT. The requirements of this approach are to identify a minimal cluster that embeds essential molecule–substrate interactions and a proper way to optimize its geometry. The NCH₃-Cu₂ case fulfills the above criterion because the two Cu adatoms effectively decouple the interactions between the NCH₃ and the flat Cu substrate. The OCH₃-Cu₃ case is somewhat different; not just two Cu adatoms but also a substrate Cu atom is included, indicating three contributing O–Cu bonds. In both cases, the cluster geometries are directly taken from DFT-optimized structures in the periodic boundary conditions. While the validity borderline of using a cluster to represent an adsorbate–surface system is always a matter of contention, our combined MO(energy)//DFT(geometry) approach delineates a way of using a small cluster for surface–cluster analogy and provides a route to predict IEs of surface molecules from its adsorption structure. This method could be particularly suitable when substrate adatoms are involved in bonding to surface adsorbates: a situation where the valence electrons of the adsorbate molecule are well-localized in a minimal cluster.

ASSOCIATED CONTENT

Supporting Information

Details of MOs of NCH₃-Cu₂, structures, and LDOS of OCH₃ on Cu clusters, and all authors' names in ref 40. This material is available free of charge via the Internet at <http://pubs.acs.org>.

AUTHOR INFORMATION

Corresponding Authors

*E-mail: wpai@ntu.edu.tw. Tel: +886-2-33665252 (W.W.P.).
*E-mail: amtyh@ntu.edu.tw. Tel: +886-2-33665250 (M.H.).

Notes

The authors declare no competing financial interest.

ACKNOWLEDGMENTS

This work is supported by the Ministry of Science and Technology (Taiwan) (102-2113-M-002-006) and the National Taiwan University Excellence Research Program (103R890921).

REFERENCES

- (1) Chen, P. T.; Pai, W. W.; Chang, S. W.; Hayashi, M. Scanning Tunneling Microscopy and Density Functional Theory Studies of Adatom-Involved Adsorption of Methylnitrene on Copper (110) Surface. *J. Phys. Chem. C* **2013**, *117*, 12111–12116.
- (2) Gomes, J. R. B.; Bofill, J. M.; Illas, F. Azomethane Decomposition Catalyzed by Pt(111): An Example of Anti-Bronsted–Evans–Polanyi Behavior. *J. Phys. Chem. C* **2008**, *112*, 1072–1080.
- (3) Díaz-Requejo, M. M.; Pérez, P. J. Coinage Metal Catalyzed C–H Bond Functionalization of Hydrocarbons. *Chem. Rev.* **2008**, *108*, 3379–3394.
- (4) Zhai, R. S.; Chan, Y. L.; Hsu, C. K.; Chuang, P.; Klauser, R.; Chuang, T. J. Generation and Spectroscopic Characterization of Methylnitrene Diradicals Adsorbed on the Cu(110) Surface. *ChemPhysChem* **2004**, *5*, 1038–1041.
- (5) Pai, W. W.; Chan, Y. L.; Chuang, T. J. Chemisorption of Methyl (CH_3) and Methylnitrene (NCH_3) Radicals on Cu Surfaces Studied by STM and LEED. *Chin. J. Phys.* **2005**, *43*, 212–218.
- (6) Pai, W. W.; Chan, Y. L.; Chang, S. W.; Chuang, T. J.; Lin, C. H. Adsorption of Methyl (CH_3) and Methylnitrene (NCH_3) Radicals on Cu Surfaces Studied by Scanning Tunneling Microscopy. *Jpn. J. Appl. Phys.* **2006**, *45*, 2372–2376.
- (7) Berry, R. S. Electronic Structure and Spectra of NH and Nitrenes. In *Nitrenes*; Lwowski, W., Ed.; Wiley-Interscience: New York, 1970; pp 13–45.
- (8) Bent, B. E. Mimicking Aspects of Heterogeneous Catalysis: Generating, Isolating, and Reacting Proposed Surface Intermediates on Single Crystals in Vacuum. *Chem. Rev.* **1996**, *96*, 1361–1390.
- (9) Yarkony, D. R.; Schaefer, H. F., III; Rothenberg, S. X. $^3\text{A}_2$, a ^1E , and $b^1\text{A}_1$ Electronic States of Methylnitrene. *J. Am. Chem. Soc.* **1974**, *96*, 5974–5977.
- (10) Demuynck, J.; Fox, D. J.; Yamaguchi, Y.; Schaefer, H. F., III. Triplet Methylnitrene: An Indefinitely Stable Species in the Absence of Collisions. *J. Am. Chem. Soc.* **1980**, *102*, 6204–6207.
- (11) Pople, J. A.; Raghavachari, K.; Frisch, M. J.; Binkley, J. S.; Schleyer, P. v. R. Comprehensive Theoretical Study of Isomers and Rearrangement Barriers of Even-Electron Polyatomic Molecules H_mABH_n (A, B = carbon, nitrogen, oxygen, and fluorine). *J. Am. Chem. Soc.* **1983**, *105*, 6389–6398.
- (12) Dickens, J. E.; Irvine, W. M.; Devries, C. H. Hydrogenation of Interstellar Molecules: A Survey for Methylenimine (CH_2NH). *Astrophys. J.* **1997**, *479*, 307–312.
- (13) Rimola, A.; Sodupe, M.; Ugliengo, P. Computational Study of Interstellar Glycine Formation Occurring at Radical Surfaces of Water-Ice Dust Particles. *Astrophys. J.* **2012**, *754*, 24.
- (14) Carrick, P. G.; Engelking, P. C. Electronic Emission Spectrum of Methylnitrene. *J. Chem. Phys.* **1984**, *81*, 1661–1665.
- (15) Ferrante, R. F. Spectroscopy of Matrix-Isolated Methylnitrene. *J. Chem. Phys.* **1987**, *86*, 25–32.
- (16) Carrick, P. G.; Brazier, C. R.; Bernath, P. F.; Engelking, P. C. The Structure of the Methylnitrene Radical. *J. Am. Chem. Soc.* **1987**, *109*, 5100–5102.
- (17) Chappell, E. L.; Engelking, P. C. Methylnitrene Free Radical. Ground State Vibrational Fundamentals and Harmonic Force Field from Jet-Cooled Emission Spectra of the A^3E – X^3A_2 Band System. *J. Chem. Phys.* **1988**, *89*, 6007–6016.
- (18) Shang, H.; Yu, C.; Ying, L.; Zhao, X. Investigation of the A^3E – X^3A_2 System of Methylnitrene Radical by Laser Spectroscopy. *J. Chem. Phys.* **1995**, *103*, 4418–4426.
- (19) Ying, L.; Xia, Y.; Shang, H.; Zhao, X.; Tang, Y. Photo-dissociation of Methylazide: Observation of Triplet Methylnitrene Radical. *J. Chem. Phys.* **1996**, *105*, 5798–5805.
- (20) Shang, H.; Gao, R.; Ying, L.; Zhao, X.; Tang, Y. Laser Induced Dispersed Fluorescence Spectra of CH_3N Radical and the Lifetime of Its A^3E State. *Chem. Phys. Lett.* **1997**, *267*, 345–350.
- (21) Nguyen, M. T. Singlet $1\text{A}''$ Methylnitrene: A Possible Intermediate in the Photochemical Decomposition of Methylazide. *Chem. Phys. Lett.* **1985**, *117*, 290–294.
- (22) Richards, C., Jr.; Meredith, C.; Kim, S. J.; Quelch, G. E.; Schaefer, H. F., III. Is There a Potential Minimum Corresponding to Singlet Methylnitrene? A Study of the CH_3N to CH_2NH Rearrangement on the Lowest Singlet-State Potential-Energy Hypersurface. *J. Chem. Phys.* **1994**, *100*, 481–489.
- (23) Kemnitz, C. R.; Ellison, G. B.; Karney, W. L.; Borden, W. T. CASSCF and CASPT2 Ab Initio Electronic Structure Calculations Find Singlet Methylnitrene Is an Energy Minimum. *J. Am. Chem. Soc.* **2000**, *122*, 1098–1101.
- (24) Wang, J.; Sun, Z.; Zhu, X.; Yang, X.; Ge, M. F.; Wang, D. The CH_3N Diradical: Experimental and Theoretical Determinations of the Ionization Energies. *Angew. Chem., Int. Ed.* **2001**, *40*, 3055–3057.
- (25) Hou, C. Y.; Zhang, H. X.; Sun, C. C. Ab Initio Study of the Spectroscopy of CH_3N and $\text{CH}_3\text{CH}_2\text{N}$. *J. Phys. Chem. A* **2006**, *110*, 10260–10266.
- (26) Muetterties, E. L.; Rhodin, T. N.; Band, E.; Brucker, C. F.; Pretzer, W. R. Clusters and Surfaces. *Chem. Rev.* **1979**, *79*, 91–137.
- (27) Bagus, P. S.; Wieckowski, A.; Wöll, C. Ionic Adsorbates on Metal Surfaces. *Int. J. Quantum Chem.* **2010**, *110*, 2844–2859.
- (28) Walter, M.; Frondelius, P.; Honkala, K.; Häkkinen, H. Electronic Structure of MgO-Supported Au Clusters: Quantum Dots Probed by Scanning Tunneling Microscopy. *Phys. Rev. Lett.* **2007**, *99*, 096102.
- (29) Hermann, K.; Bagus, P. S.; Nelin, C. J. Size Dependence of Surface Cluster Models: CO Adsorbed on Cu(100). *Phys. Rev. B* **1987**, *35*, 9467–9473.
- (30) Perdew, J. P.; Wang, Y. Accurate and Simple Analytic Representation of the Electron-Gas Correlation Energy. *Phys. Rev. B* **1992**, *45*, 13244–13249.
- (31) Kresse, G.; Hafner, J. Ab Initio Molecular Dynamics for Open-Shell Transition Metals. *Phys. Rev. B* **1993**, *48*, 13115–13118.
- (32) Kresse, G.; Furthmüller, J. Efficient Iterative Schemes for Ab Initio Total-Energy Calculations Using a Plane-Wave Basis Set. *Phys. Rev. B* **1996**, *54*, 11169–11186.
- (33) Kresse, G.; Furthmüller, J. Efficiency of Ab Initio Total Energy Calculations for Metals and Semiconductors Using a Plane-Wave Basis Set. *Comput. Mater. Sci.* **1996**, *6*, 15–50.
- (34) Monkhorst, H. J.; Pack, J. D. Special Points for Brillouin-Zone Integrations. *Phys. Rev. B* **1976**, *13*, 5188–5192.
- (35) Curtiss, L. A.; Raghavachari, K.; Pople, J. A. Gaussian-2 Theory Using Reduced Møller-Plesset Orders. *J. Chem. Phys.* **1993**, *98*, 1293–1298.
- (36) Gronert, S. Theoretical Studies of Proton Transfers. 1. The Potential Energy Surfaces of the Identity Reactions of the First- and Second-Row Non-Metal Hydrides with Their Conjugate Bases. *J. Am. Chem. Soc.* **1993**, *115*, 10258–10266.
- (37) Hay, P. J.; Wadt, W. R. Ab Initio Effective Core Potentials for Molecular Calculations. Potentials for the Transition Metal Atoms Sc to Hg. *J. Chem. Phys.* **1985**, *82*, 270–283.
- (38) Wadt, W. R.; Hay, P. J. Ab Initio Effective Core Potentials for Molecular Calculations. Potentials for the Transition Metal Atoms Na to Bi. *J. Chem. Phys.* **1985**, *82*, 284–298.
- (39) Hay, P. J.; Wadt, W. R. Ab Initio Effective Core Potentials for Molecular Calculations. Potentials for K to Au Including the Outermost Core Orbitals. *J. Chem. Phys.* **1985**, *82*, 299–310.

- (40) Frisch, M. J.; Trucks, G. W.; Schlegel, H. B.; Scuseria, G. E.; Robb, M. A.; Cheeseman, J. R.; Montgomery, J. A., Jr.; Vreven, T.; Kudin, K. N.; Burant, J. C.; et al. *Gaussian 03*, Revision C.02; Gaussian, Inc: Wallingford, CT, 2004. See all authors' names in the Supporting Information.
- (41) Besenbacher, F.; Nørskov, J. K. Oxygen Chemisorption on Metal Surfaces: General Trends for Cu, Ni and Ag. *Prog. Surf. Sci.* **1993**, *44*, 5–66.
- (42) Pai, W. W.; Reutt-Robey, J. E. Formation of ($n \times 1$)-O/Ag(110) Overlayers and the Role of Step-Edge Atoms. *Phys. Rev. B* **1996**, *53*, 15997.
- (43) Bradley, M. K.; Kreikemeyer Lorenzo, D.; Unterberger, W.; Duncan, D. A.; Lerotholi, T. J.; Robinson, J.; Woodruff, D. P. Methoxy Species on Cu(110): Understanding the Local Structure of a Key Catalytic Reaction Intermediate. *Phys. Rev. Lett.* **2010**, *105*, 086101.
- (44) Kreikemeyer Lorenzo, D.; Bradley, M. K.; Unterberger, W.; Duncan, D. A.; Lerotholi, T. J.; Robinson, J.; Woodruff, D. P. The Structure of Methoxy Species on Cu(110): A Combined Photoelectron Diffraction and Density Functional Theory Determination. *Surf. Sci.* **2011**, *605*, 193–205.
- (45) Hofmann, P.; Schindler, K. M.; Bao, S.; Fritzsche, V.; Ricken, D. E.; Bradshaw, A. M.; Woodruff, D. P. The Geometric Structure of the Surface Methoxy Species on Cu(111). *Surf. Sci.* **1994**, *304*, 74–84.
- (46) Bowker, M.; Madix, R. J. XPS, UPS and Thermal Desorption Studies of Alcohol Adsorption on Cu(110). *Surf. Sci.* **1980**, *95*, 190–206.
- (47) Sexton, B. A.; Hughes, A. E.; Avery, N. R. A Spectroscopic Study of the Adsorption and Reactions of Methanol, Formaldehyde and Methyl Formate on Clean and Oxygenated Cu(110) Surfaces. *Surf. Sci.* **1985**, *155*, 366–386.